

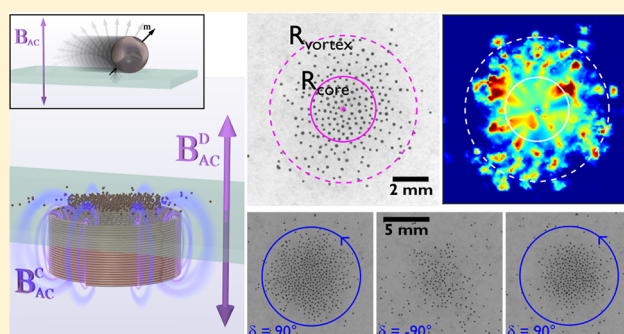
Guided Self-Assembly and Control of Vortices in Ensembles of Active Magnetic Rollers

 Gašper Kokot,^{†,‡} Andrey Sokolov,[‡] and Alexey Snezhko^{*,‡,†}
[†]Northwestern Argonne Institute of Science and Engineering (NAISE), Engineering Science and Applied Mathematics, Northwestern University, Evanston, Illinois 60208, United States

[‡]Materials Science Division, Argonne National Laboratory, Lemont, Illinois 60439, United States

Supporting Information

ABSTRACT: Active magnetic colloids are capable of rich collective behavior and complex self-organization. The interplay between short- and long-range interactions taking place away from equilibrium often results in a spontaneous formation of localized dynamic microstructures. Here we report a method for guided self-assembly and control of self-organized colloidal vortices emerging in a ferromagnetic particle ensemble energized by a uniaxial alternating (ac) magnetic field. The structure of a vortex composed of rolling magnetic particles can be stabilized and manipulated by means of an additional strongly localized alternating magnetic field provided by a minicoil. By tuning the parameters of the localized field, we effectively control the dimensions and particle number density in the vortex. We find that the roller vortex self-organization is assisted by field-induced magnetic “steering” rather than magnetic field gradients and is only possible while the system is in the active (magnetic rollers) state. We demonstrate that parameters of the emergent vortex are efficiently tuned by a phase shift between alternating magnetic fields. The method for assisted self-organization of rolling magnetic colloids into a vortex with on-demand characteristics suggests a new tool for active matter control and manipulation that may lead to a development of new approaches toward the guided microscopic transport in active particle systems.



INTRODUCTION

Active particles are self-propelled units which are powered by the energy stored in the environment or provided by external fields. There are two major classes of active systems: biological agents (from microorganisms and insects to animals and people)^{1–5} and synthetic agents (ranging from self-propelled microparticles to robots and vehicles).^{6–14} While mechanisms of self-propulsion may be intrinsically different, many systems show common features: transition to collective motion with the increase in concentration manifested by an emergence of large-scale flows, vortices, and coherent dynamics structures.^{15,16}

The complexity of the observed collective behavior originates from a fine interplay between long- and short-range interparticle interactions, and noise in the system.^{17–20} Because of an out-of-equilibrium nature and high degree of stochasticity in active systems, a fine control of emerged large-scale structures on an individual level is a challenging task. Emerged dynamic states (vortices, flocks, and flows) may randomly self-organize, disintegrate, or travel through the system. However, the motion of active particles can often be rectified and ordered by specifically designed geometrical constrains. A stationary system of active vortices could be induced in hollow wells^{21–23} or imposed by a microscopic pillar array.²⁴ Soft gravitational confinements could be

efficiently used to constrain and stabilize a magnetic roller vortex.^{25,26} Although the above approaches may effectively enforce a positional order of the self-organized vortices, they provide no tunability. Once formed, the vortices maintain positions, order, and sizes. Introduction of the additional reconfigurable fields into the system allows overcoming such limitations and creates the possibility of on-demand structures with adjustable characteristics.

In this article, we report a new method for the controlled self-assembly of localized vortices composed of active ferromagnetic rollers energized by a uniform uniaxial ac magnetic field. The method relies on the use of an additional tightly localized in space ac magnetic field with a relatively small amplitude (fraction of the driving magnetic field). We characterize the emerged vortex and demonstrate the reversibility of its configurations in response to changes in the parameters of the localized magnetic field. Finally, we explore the underlying mechanism of the vortex self-organization and dynamics in the presence of a local field

Special Issue: Advances in Active Materials

Received: September 25, 2019

Revised: November 15, 2019

Published: November 22, 2019

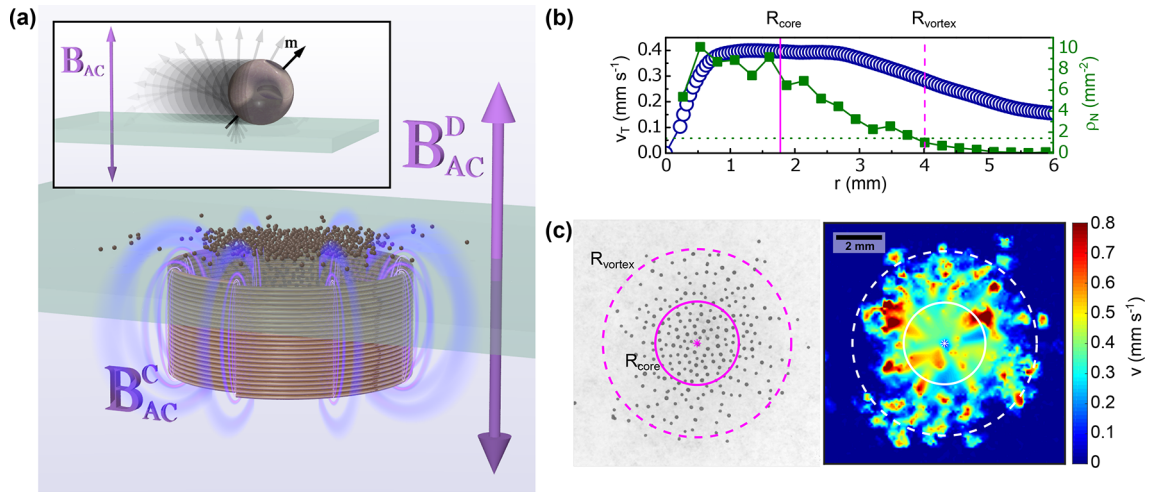


Figure 1. (a) Schematics of the experimental setup. (Inset) Rolling of a spherical magnetic particle with a permanent magnetic moment \mathbf{m} in the ac vertical magnetic field. (Main panel) A small solenoid (ferritic core is not shown) creates a nonuniform local magnetic field and traps the rollers. (b) Azimuthally averaged tangential velocity v_r profile (left axis, blue open circles) and particle number density ρ_N (right axis, green squares) in a vortex versus the distance from the vortex center r . The green dotted horizontal line indicates the selected cutoff $\rho_N = 1.4 \text{ mm}^{-2}$. The solid and dashed magenta vertical lines mark the core radius R_{core} and the vortex radius R_{vortex} . (c) Snapshot of particles in the vortex (left) and vortex velocity field (right) as obtained by particle image velocimetry. Dashed and solid lines encircle the core and the vortex, respectively.

nonuniformity and show that it stems from the motility of the active magnetic particles. The discovered mechanism is new and differs from the one reported earlier for active magnetic roller systems,²⁶ where passive scatterers were used to adjust the dynamics of the vortex structure.

EXPERIMENTAL SECTION

Ferromagnetic nickel spheres with a diameter of $137 \pm 13 \mu\text{m}$ (Alfa Aesar) were magnetized with a rare-earth permanent magnet (0.5 T). The average remnant magnetic moment per particle is $|\mathbf{m}| = 2 \times 10^{-8} \text{ A m}^2$. The particles were then placed into a flat-bottomed glass container filled with isopropanol. A pair of Helmholtz coils (20 cm in diameter) was positioned around the container to create a uniaxial homogeneous oscillating magnetic field $\mathbf{B}^D = B_0^D \sin(2\pi f_B t) \mathbf{z}_0$ perpendicular to the bottom of the container, where B_0^D and f_B are respectively the amplitude and frequency of the driving field. In a certain range of the driving field parameters, the particles spontaneously break the symmetry of a rocking motion with the external driving field and start a steady rotation.^{25,27} In the presence of the interface (solid bottom of the container), a steady particle rotation leads to a horizontal displacement: rolling (Figure 1a inset). The initial direction of the rolling of each particle is selected randomly since the uniaxial magnetic field is used (no-rotational field) to energize the system. The rolling direction may change because of particle shape irregularities or as a result of interparticle interactions. In the course of rolling, each particle generates strong hydrodynamic flows. The magnetic and hydrodynamic interactions of particles lead to self-organization into dynamic flocks and vortices in a certain range of the excitation field parameters and above a certain critical particle number density.²⁵ The frequency of the driving field $f_B = 40 \text{ Hz}$ was selected to promote a stable vortex phase in the system.^{25,26}

A small solenoid with a ferritic core was mounted under the bottom (2 mm thick) of the container (Figure 1a). The radius of the solenoid coil $R_{\text{coil}} = 3.9 \text{ mm}$ and the total length of $L_{\text{coil}} = 10 \text{ mm}$ were chosen to be comparable with the size of vortices emerging in the active magnetic roller system. The solenoid was energized by a separate power supply to create a nonuniform ac magnetic field \mathbf{B}^C in a small area above the solenoid. For the sake of simplicity, we characterize the magnetic field \mathbf{B}^C by the maximum value of its vertical component measured with a Hall probe at the bottom of the glass container (2 mm above the coil; see the sketch in Figure 1a, main panel) $B^C = B_0^C \sin(2\pi f_B t + \delta)$. The field amplitude B_0^C and the phase shift δ relative to

\mathbf{B}^D are the main parameters used to control the emerged vortex. Importantly, even if the solenoid is not energized, the presence of the ferritic core modifies the uniform magnetic field \mathbf{B}^D generated by the pair of driving coils, creating a perturbation \mathbf{B}^f . Correspondingly, the total magnetic field may be represented as $\mathbf{B} = \mathbf{B}^D + \mathbf{B}^f + \mathbf{B}^C$, where the first two terms are proportional to the current in the large coils.

The dynamics of the emerged vortex was recorded with a fast CMOS camera (IDT, 60 fps, 0.013 mm/pixel at 0.16 \times magnification) mounted on a stereomicroscope (Leica). The velocity field of the magnetic roller vortices was extracted from the sequence of images by a standard PIV (particle image velocimetry) technique using the MatPIV package for Matlab. The position of the vortex “eye” was detected by finding the local minimum/maximum of the magnitude of the velocity/vorticity field. For the characterization of the vortex spatiotemporal configuration, we determine the core and vortex radii, vortex angular velocity, and pair distribution function. The vortex core radius R_{core} was defined as an average of all radii at which the tangential velocities were larger than 0.95 of the maximal measured velocity (solid lines in Figure 1b,c). The rotation of a vortex core resembles a “solid” body rotation. The vortex radius R_{vortex} was defined as the distance at which the particle number density, ρ_N , decreased below a selected threshold of 1.4 mm^{-2} (corresponding to 0.02 area fraction) shown as dashed lines in Figure 1b,c. The vortex angular velocity $\omega = \frac{1}{N} \sum_{i=1}^N \frac{v_{T_i}}{r_i}$ was estimated as an average of angular velocities of all particles within the vortex core, where v_{T_i} is the tangential component of a particle velocity and r_i is the distance from the vortex center. Similarly, the pair correlation function $g(r)$, which reflects the probability of finding a particle at a distance r from a reference particle, was calculated only for the particles within the core. R_{vortex} , ω , and $g(r)$ under the same experimental condition were additionally averaged over 400 realizations.

RESULTS AND DISCUSSION

Hydrodynamic and magnetic interactions in the system of magnetic rolling colloids lead to the emergence of a collective motion and large-scale coherent structures (flocks, clusters, and vortices) in a certain range of excitation parameters.^{25,26,28} However, the onset of collective behavior requires the local particle number density to be above a critical threshold, which is often hard to achieve in a spatially unconstrained system. In

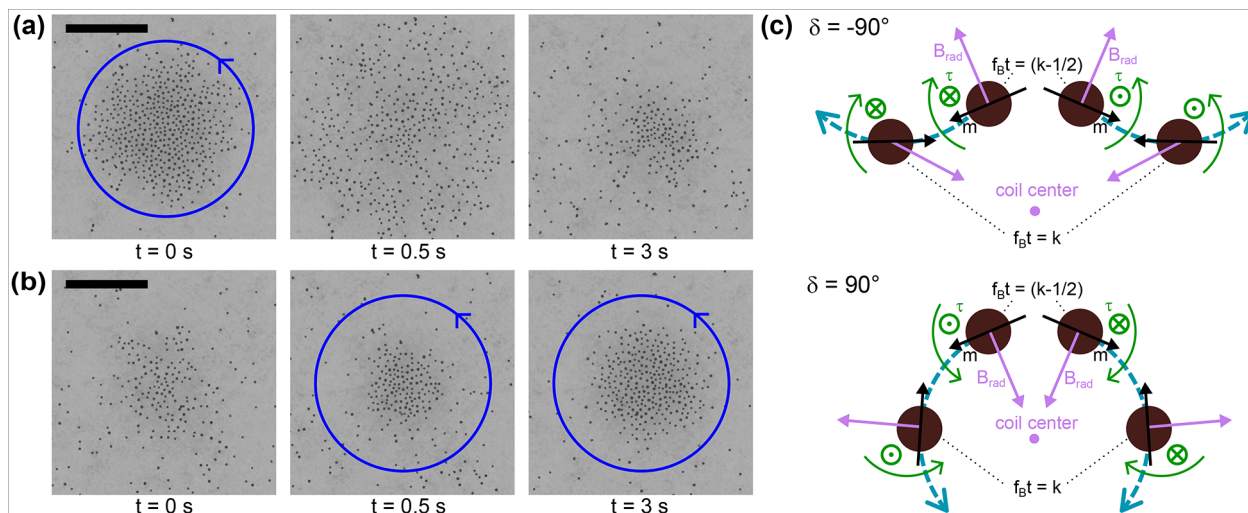


Figure 2. Vortex formation and disassembly in response to changes in phase shift δ . (a) A series of snapshots illustrate the disassembly of an initially stable roller vortex. The phase shift between the driving field and the small solenoid field, δ , was changed from 90 to -90° at $t = 0$. (b) Reassembly of a vortex. δ was changed from -90 to 90° at $t = 0$. For both (a) and (b), the scale bars are 5 mm, $B_0^D = 8.59$ mT, and $B_0^C = 0.15$ mT. See also Supporting Information Video S1. (c) Schematic illustration of the magnetic steering mechanism. The radial component of \mathbf{B}_C , marked as B_{rad} (magenta arrow), applies a torque (shown green) pointing in or out of the plane of the panel to steer the particle with the magnetic moment \mathbf{m} (black arrow). Regardless of the initial particle orientation, the steering direction is either away from the solenoid center (top panel) for $\delta = -90^\circ$ or toward it (bottom panel) for $\delta = 90^\circ$, for all rolling directions (the left and right sides of each panel) and at all t values (compare top and bottom particles shifted half of a field period in time). The sketches demonstrate the vector orientation at instances of maximal torque at each period $f_B t = k$ and half-period $f_B t = k \mp 1/2$ for integer k .

our experiments we demonstrated that the field created by the additional solenoid may locally confine the motion of rollers and effectively constrain the system (soft confinement because particles still have a chance to leave the region). Importantly, such a constraint may be adjusted in the course of the experiment. The soft confinement of particles by local magnetic field inhomogeneities leads to an increase in the local particle number density and triggers self-organization into a stable vortex with controllable characteristics (Figure 2 and Videos S1 and S2). The chirality of the resulting vortex (clockwise or counterclockwise rotations) is spontaneously selected by the system. The magnetic field of the small coil \mathbf{B}^C stabilizes the structure of the vortex by preventing the loss of the particles to the gas phase and restricting the motion of the vortex core that might destabilize the structure and lead to a spontaneous transition to a flocking state.²⁶ To elucidate the mechanisms of self-organization, we tested the system behavior in a wide range of parameters within the solenoid technical specifications $B_0^C = 0 \dots 0.4$ mT and phase shifts $\delta = -180^\circ \dots +180^\circ$ while the frequency was fixed at $f_B = 40$ Hz to support the stable rolling of the magnetic particles. The range of the driving field amplitude B_0^D was between 8.5 and 9.5 mT. The amplitude of perturbation field \mathbf{B}^f induced by the ferritic core was around 1 mT at the bottom of the container. No significant effects of the earth's magnetic field on the motion of rollers have been detected.

When the small solenoid is energized and \mathbf{B}^C is in phase with the driving field ($\delta = 0^\circ$), the rollers start to concentrate around the solenoid center, and when enough particles are accumulated, a roller vortex spontaneously emerges. However, when \mathbf{B}^C is below a certain threshold, the vortex is not in a stable state: particles constantly leave or join the area above the small solenoid, and the vortex is transient as it perpetually falls apart and reassembles. We found that a stable vortex requires amplitudes above $B_0^C = 0.1$ mT at $\delta = 0^\circ$. The field of the

secondary coil alone is not enough to nucleate the vortex. To fix the number of particles in the vortex n , all particles not involved in the vortex were removed from the system with a pipet. The radius of the stable vortex R_{vortex} at $\delta = 0^\circ$ is not affected by changes in the field amplitude B_0^C (Figure 3a, red

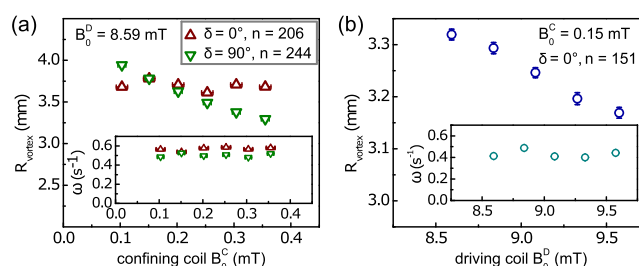


Figure 3. Dependence of the vortex radius and the angular velocity ω on (a) the small coil magnetic field B_0^C and (b) the driving magnetic field B_0^D . Magnetic rollers not involved in the roller vortex were removed from the system to keep the number of particles, n , in the vortex constant.

triangles). The increase in the driving field amplitude B_0^D and, correspondingly, B^f slightly decreases the vortex size (Figure 3b) as a result of an increase in the field gradients pushing the particles closer to the center of the ferritic core. If the phase shift is changed to $\delta = 90^\circ$, then the vortex behavior becomes dramatically different. In this case, the increase in B_0^C makes the vortex much tighter, while the angular velocity ω remains the same (Figure 3a, green triangles). At amplitudes of the field above 0.4 mT, the particles in the center of the roller vortex become too close to each other, triggering clustering of the rollers and destruction of the collective vortical motion.

The assembly of a roller vortex in the presence of the steering coil occurs only for $-30^\circ < \delta < 210^\circ$ with the highest stability achieved at $\delta = 90^\circ$. Switching the phase between $\delta =$

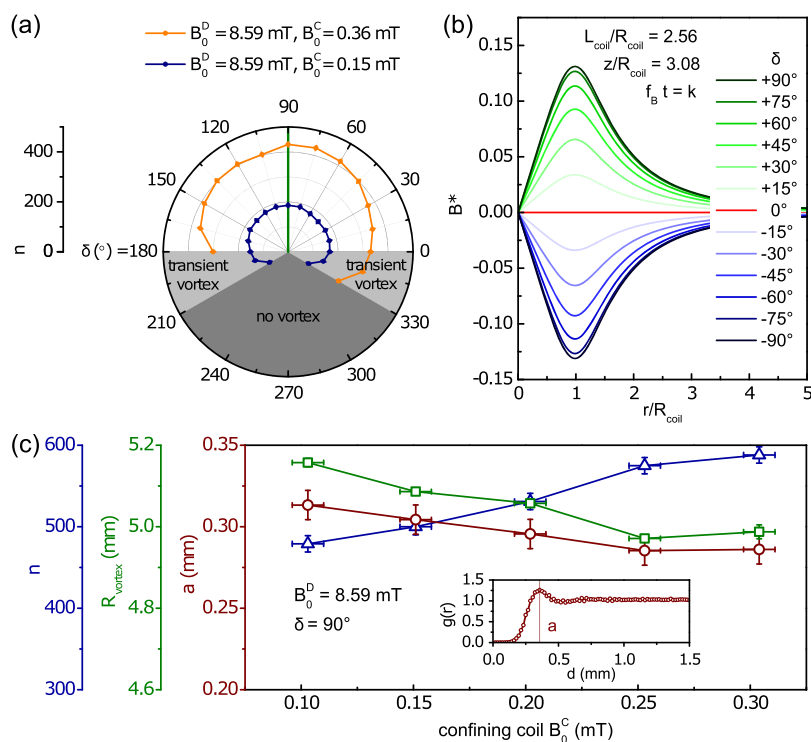


Figure 4. Manipulation of a vortex structure. (a) Number of the particles n confined in the roller vortex as a function of the phase shift δ . The green line marks the peak in n . (b) Numerical calculation of the normalized amplitude of the radial field component of $B^* = B_{rad}^C/(\mu NI)$ of a finite solenoid ($L_{coil}/R_{coil} = 2.56$) at the surface of the glass container ($z/R_{coil} = 3.08$) for $f_B t = k$ plated as a function of the normalized distance from the solenoid axis r/R_{coil} . The maximum peak at $\delta = 90^\circ$ corresponds to the maximum of n in (a). (c) Number of particles, n , confined in a vortex, vortex radius R_{vortex} and a characteristic interparticle spacing, a , in the active roller vortex as a function of the steering solenoid field amplitude B_0^C .

90° and -90° in the course of the experiment results in either the formation or disassembly of the vortex, proceeding through the capture or release of the rollers, respectively (Figure 2 and Supporting Information Video S1). The observed vortex behavior and its nontrivial response to changes in the phase shift, δ , stem from the mechanism of the roller vortex self-organization. The system is active (magnetic particles are self-propelling) by nature, and the formation of vortices originates from the activity and aligning interactions between rollers facilitated by magnetic and hydrodynamic coupling.^{25,28} In case the roller trapping mechanism is facilitated only by a local magnetic field gradient, the strongest pull toward the center of the solenoid due to the nonuniformity of \mathbf{B} is expected to be achieved at $\delta = 0$. However, the vortex is most stable at $\delta = 90^\circ$. To explain this experimental observation, we analyze the motion of an individual roller and its interaction with the magnetic fields.

As previously demonstrated,²⁵ internal magnetic moments of rollers rotate in synchrony with the driving alternating magnetic field \mathbf{B}^D : the spinning magnetic moments are vertical when \mathbf{B}^D is maximized and horizontal when $\mathbf{B}^D = 0$. Therefore, for $\delta = 90^\circ$, the solenoid field B^C is maximized when the magnetic moments or rollers are horizontal. The radial component of \mathbf{B}^C acts on the magnetic moment of the roller \mathbf{m} , which results in a torque $\boldsymbol{\tau} = \mathbf{m} \times \mathbf{B}^C$ that steers the magnetic particles inward toward the vortex for $\delta = 90^\circ$ or outward for $\delta = -90^\circ$ for both clockwise and counterclockwise vortices (Figure 2c). The response of the system is immediate, and the phase reversal can be efficiently used to create the vortex on demand. The analysis of the obtained experimental data shows that the primary mechanism of the rollers'

confinement and subsequent formation of a vortex is synchronized magnetic particle steering rather than a gradient attraction. The robust steering is possible only when frequencies of both driving and solenoid fields are equal and the phase shift δ between them is constant.

To obtain detailed insights into the process of directed vortex self-organization and to develop a general method of vortex control after dynamic self-assembly, we performed a set of additional experiments with a significantly larger number of rollers in the container in a gas roller phase than the number of particles that could be potentially confined by the steering coil to form a spontaneous vortex. The rollers were uniformly distributed over the container and freely moved around the self-assembled vortex at an approximate number density of 0.4 mm^{-2} . Such an experimental configuration allowed us to directly observe the trapping and release of particles in response to the changes of the phase shift δ and B^C .

The maximal number of particles confined by the small coil and forming a vortex is observed for δ close to the optimal value of 90° (Figure 4a and Supporting Information Figure S1). When the phase shift approaches 0 or 180° , a large number of particles leave the vortex, followed by a 30° range with transient vortices only. To gain detailed insight into this behavior and the torques acting on the rollers, we calculate the dimensionless radial field component²⁹ $B^* = B_{rad}^C/(\mu NI)$, where μ is magnetic permeability of the ferritic core, N is the number of turns, and I is the ac current amplitude through the solenoid. We perform the numerical calculations of the radial field components for a plane at the position of the rollers, above the small solenoid ($z/R_{coil} = 3.08$, where the origin is placed in the center and the z axis is aligned with the solenoid

axis), for different δ values to determine the direction and the amplitude of the radial field. For clarity, we present only results calculated at a specific moment in the field's oscillation cycle when the steering torques are maximal at $\mathbf{B}^D + \mathbf{B}^f = 0$ (i.e., $\sin(2\pi f_B t) = 0$, or, more specifically, when $f_B t = k$ for any integer k). As we can see in Figure 4b, B^* is zero at the central axis of the solenoid, which coincides with the vortex eye and has a maximum at R_{coil} . As a consequence, τ exhibits the strongest steering close to R_{coil} and no steering at the center of the vortex. The number of particles in the vortex, n , drastically decreases for $0 > \delta > 180^\circ$ because the steering torque τ drives rollers away from the solenoid central axis, yet some rollers remained in an area close to the center where steering torques are negligible. Spontaneous self-assembly of the roller vortex still occurs, provided a local particle number density is above a threshold. When B^* is further increased in the regime of "outward" steering ($210 < \delta < 330^\circ$), no vortex was observed (Figure 4a). The onset of the effective magnetic steering of active rollers is observed at $B_0^C = 0.1$ mT, which is a tiny fraction of the driving field amplitude. This corresponds in our system to only ~ 2 nNm steering torque defined at the B^* peak value that is sufficient for the effective steering of a roller.

For the characterization of particle ordering in the vortex stabilized by a steering coil, we calculated the pair correlation function $g(r)$ for the rollers in the vortex core (Figure 4c, inset). The presence of short-range order in the vortex is manifested by a well-defined peak in $g(r)$. A characteristic interparticle distance in the vortex, a , is determined from the position of this peak. The structure of the self-organized vortex formed at optimal $\delta = 90^\circ$ can be further manipulated by the amplitude of the steering coil B_0^C . At each value of B_0^C , we determined the vortex radius R_{vortex} , the number of particles trapped in the vortex n , and the typical distance between particles a (Figure 4c). In contrast to the previous set of experiments, where the roller gas was removed from the system, the number of particles in the vortex n is increasing. Remarkably, while the number of particles involved in the vortex n increases with the field amplitude B_0^C , the vortex size R_{vortex} decreases. The latter is accompanied by a shortening of a , which eventually leads to clustering in the vortex core. Active magnetic rollers begin to form clusters when the particle number density reaches 12.5 mm^{-2} . This process triggers the demagnetization of the rollers locked in the clusters and inevitably leads to the vortex disassembly.

SUMMARY AND CONCLUSIONS

We introduced a new approach to controlling and manipulating the complex dynamics of active magnetic colloids. Although the uniform magnetic field energizes the particles, turning them into rollers and driving the ensemble away from equilibrium, an independent, much smaller in amplitude localized ac magnetic field enables guided self-assembly of particles into a dynamic vortex with a spontaneously selected chirality. Our studies reveal that the size of the emerged vortices and the number of particles involved are controlled by the amplitude of the local field and the phase shift between the driving and local fields. We find that the roller vortex self-organization is assisted by a field-induced magnetic "steering", relying on the activity of the particles, and does not originate from the local magnetic field gradients. The new mechanism allows the use of significantly smaller fields to control the active vortex structure and dynamics. The fast response of the vortex to changes in the magnetic field parameters enables the

assembly of vortices with on-demand adjustable characteristics. This new approach may be further extended toward the systems of multiple self-assembled vortices independently controlled by a lattice of microsolenoids enabling the design of complex active multivortex states in colloidal ensembles for the purpose of targeted cargo transport or controlled localized mixing.

ASSOCIATED CONTENT

Supporting Information

Supporting Information is available online. The Supporting Information is available free of charge at <https://pubs.acs.org/doi/10.1021/acs.langmuir.9b03023>.

Manipulation of a vortex structure by means of a phase shift between the excitation magnetic fields (PDF)

Vortex formation and decay as a response to the change in δ (shown at twice the real time rate) (AVI)

Vortex formation and decay as a response to the change in δ (shown at a quarter of the real time rate) (AVI)

Vortex size control with changes in B_0^C (shown at twice the real time rate) (AVI)

Vortex size control with changes in B_0^C (shown at a quarter of the real time rate) (AVI)

Demonstration of steering for two particles (AVI)

AUTHOR INFORMATION

Corresponding Author

*E-mail: snezhko@anl.gov.

ORCID

Alexey Snezhko: 0000-0001-5634-6228

Notes

The authors declare no competing financial interest.

ACKNOWLEDGMENTS

The research was supported by the U.S. Department of Energy, Office of Science, Basic Energy Sciences, Materials Sciences, and Engineering Division. The authors thank Andrej Vilfan for fruitful discussions.

REFERENCES

- (1) Dombrowski, C.; Cisneros, L.; Chatkaew, S.; Goldstein, R. E.; Kessler, J. O. Self-concentration and large-scale coherence in bacterial dynamics. *Phys. Rev. Lett.* **2004**, *93*, 098103.
- (2) Couzin, I. D.; Krause, J.; Franks, N. R.; Levin, S. A. Effective leadership and decision-making in animal groups on the move. *Nature* **2005**, *433*, 513.
- (3) Grégoire, G.; Chaté, H. Onset of collective and cohesive motion. *Phys. Rev. Lett.* **2004**, *92*, 025702.
- (4) Sokolov, A.; Aranson, I. S.; Kessler, J. O.; Goldstein, R. E. Concentration dependence of the collective dynamics of swimming bacteria. *Phys. Rev. Lett.* **2007**, *98*, 158102.
- (5) Kearns, D. B. A field guide to bacterial swarming motility. *Nat. Rev. Microbiol.* **2010**, *8*, 634.
- (6) Martin, J. E.; Snezhko, A. Driving self-assembly and emergent dynamics in colloidal suspensions by time-dependent magnetic fields. *Rep. Prog. Phys.* **2013**, *76*, 126601.
- (7) Yamada, D.; Hondou, T.; Sano, M. Coherent dynamics of an asymmetric particle in a vertically vibrating bed. *Phys. Rev. E: Stat. Phys., Plasmas, Fluids, Relat. Interdiscip. Top.* **2003**, *67*, 040301.
- (8) Paxton, W. F.; Kistler, K. C.; Olmeda, C. C.; Sen, A.; St. Angelo, S. K.; Cao, Y.; Mallouk, T. E.; Lammert, P. E.; Crespi, V. H. Catalytic nanomotors: autonomous movement of striped nanorods. *J. Am. Chem. Soc.* **2004**, *126*, 13424–13431.

- (9) Snezhko, A. Complex collective dynamics of active torque-driven colloids at interfaces. *Curr. Opin. Colloid Interface Sci.* **2016**, *21*, 65–75.
- (10) Gangwal, S.; Cayre, O. J.; Velez, O. D. Dielectrophoretic assembly of metalodielectric Janus particles in AC electric fields. *Langmuir* **2008**, *24*, 13312–13320.
- (11) Massana-Cid, H.; Meng, F.; Matsunaga, D.; Golestanian, R.; Tierno, P. Tunable self-healing of magnetically propelling colloidal carpets. *Nat. Commun.* **2019**, *10*, 2444.
- (12) Liebchen, B.; Lowen, H. Synthetic Chemotaxis and Collective Behavior in Active Matter. *Acc. Chem. Res.* **2018**, *51*, 2982–2990.
- (13) Driscoll, M.; Delmotte, B. Leveraging collective effects in externally driven colloidal suspensions: Experiments and simulations. *Curr. Opin. Colloid Interface Sci.* **2019**, 4042.
- (14) Dobnikar, J. *Frontiers of Nanoscience*; Elsevier, 2019; Vol. 13; pp 23–36.
- (15) Vicsek, T.; Zafeiris, A. Collective motion. *Phys. Rep.* **2012**, *517*, 71–140.
- (16) Zöttl, A.; Stark, H. Emergent behavior in active colloids. *J. Phys.: Condens. Matter* **2016**, *28*, 253001.
- (17) Simha, R. A.; Ramaswamy, S. Hydrodynamic fluctuations and instabilities in ordered suspensions of self-propelled particles. *Phys. Rev. Lett.* **2002**, *89*, 058101.
- (18) Mohoric, T.; Kokot, G.; Osterman, N.; Snezhko, A.; Vilfan, A.; Babic, D.; Dobnikar, J. Dynamic assembly of magnetic colloidal vortices. *Langmuir* **2016**, *32*, 5094–5101.
- (19) Ngo, S.; Peshkov, A.; Aranson, I. S.; Bertin, E.; Ginelli, F.; Chaté, H. Large-scale chaos and fluctuations in active nematics. *Phys. Rev. Lett.* **2014**, *113*, 038302.
- (20) Sokolov, A.; Mozaffari, A.; Zhang, R.; de Pablo, J. J.; Snezhko, A. Emergence of Radial Tree of Bend Stripes in Active Nematics. *Phys. Rev. X* **2019**, *9*, 031014.
- (21) Lushi, E.; Wioland, H.; Goldstein, R. E. Fluid flows created by swimming bacteria drive self-organization in confined suspensions. *Proc. Natl. Acad. Sci. U. S. A.* **2014**, *111*, 9733–9738.
- (22) Wioland, H.; Woodhouse, F. G.; Dunkel, J.; Goldstein, R. E. Ferromagnetic and antiferromagnetic order in bacterial vortex lattices. *Nat. Phys.* **2016**, *12*, 341.
- (23) Bricard, A.; Caussin, J.-B.; Das, D.; Savoie, C.; Chikkadi, V.; Shitara, K.; Chepizhko, O.; Peruani, F.; Saintillan, D.; Bartolo, D. Emergent vortices in populations of colloidal rollers. *Nat. Commun.* **2015**, *6*, 7470.
- (24) Nishiguchi, D.; Aranson, I. S.; Snezhko, A.; Sokolov, A. Engineering bacterial vortex lattice via direct laser lithography. *Nat. Commun.* **2018**, *9*, 4486.
- (25) Kaiser, A.; Snezhko, A.; Aranson, I. S. Flocking ferromagnetic colloids. *Science advances* **2017**, *3*, e1601469.
- (26) Kokot, G.; Snezhko, A. Manipulation of emergent vortices in swarms of magnetic rollers. *Nat. Commun.* **2018**, *9*, 2344.
- (27) Kokot, G.; Vilfan, A.; Glatz, A.; Snezhko, A. Diffusive ferromagnetic roller gas. *Soft Matter* **2019**, *15*, 3612–3619.
- (28) Wang, Y.; Canic, S.; Kokot, G.; Snezhko, A.; Aranson, I. Quantifying hydrodynamic collective states of magnetic colloidal spinners and rollers. *Physical Review Fluids* **2019**, *4*, 013701.
- (29) Callaghan, E. E.; Maslen, S. H. The magnetic field of a finite solenoid. *NASA TN D-465*, 1960.